

Ballistic thermal conductance limited by phonon roughness scattering: A comparison of power-law and Gaussian roughness

G. Palasantzas*

Department of Applied Physics, Materials Science Center, University of Groningen, 9747 AG Groningen, The Netherlands

(Received 30 March 2004; published 22 October 2004)

In this work, we have investigated the influence of power-law roughness on the ballistic thermal conductance K_{TH} for a nanosized beam adiabatically connected between two heat reservoirs. The sideways wall beam roughness is assumed to be power-law type, which is described by the roughness amplitude w , the in-plane roughness correlation length ξ and the roughness exponent $0 \leq H \leq 1$. Distinct differences occur in between power-law and Gaussian wall roughness. For power-law roughness with low roughness exponents $H (< 0.5)$, the influence of phonon scattering can be rather destructive leading to significant deviations from the universal conductance value for flat beam walls. On the other hand for large roughness exponents ($H > 0.5$) the conductance drop is significantly smaller than that of Gaussian roughness assuming similar roughness ratios w/ξ .

DOI: 10.1103/PhysRevB.70.153404

PACS number(s): 68.35.Ct, 65.40.-b, 72.15.Eb, 74.25.Fy

Besides one-dimensional electron transport¹⁻³ that is understood within the framework of Büttiker-Landauer theory,^{4,5} one-dimensional phonon transport should also be possible. However, despite the long-standing theoretical interest in this topic,⁶ the question whether the phonon thermal conductance should be quantized in one dimension was only recently addressed theoretically and experimentally.^{7,8} Indeed, using the Landauer formulation of transport theory, it was predicted that dielectric quantum wires should exhibit quantized thermal conductance at low temperatures in a ballistic phonon regime. The quantum of thermal conductance is universal (independent of material characteristics) and equal to $K_B^2 T/3h$, where K_B is the Boltzmann constant, h is Planck's constant, and T is the temperature.

In the theory that describes the thermal conductance K_{TH} (Ref. 7) the only material and geometry dependence arises through the long wavelength cutoff frequencies of the elastic waves in the beam. As the temperature decreases T and approaching 0 K, the conductance is dominated by the lowest few modes with zero cutoff frequency. Indeed, K_{TH} approaches the universal value $K_U = N_0 K_B^2 T/3h$ with N_0 the number of modes with zero cutoff frequency at long wavelengths ($N_0=4$ for a freestanding beam).⁸ Recently, Schwab *et al.* successfully measured the universal conductance K_U in a suspended silicon nitride bridge.⁸ Their experiment shows a universal conductance $K_{\text{TH}}=K_U$ at temperatures $T < 0.08$ K, while for higher temperatures $T > 1$ K the conductance K_{TH} increases above K_U , as the modes with nonzero cutoff frequencies become excited and contribute to the heat transport. However, at intermediate temperatures $0.1 \text{ K} < T < 1 \text{ K}$ the thermal conductance is decreased below its universal value as it was shown experimentally by Schwab *et al.*,⁸ and it was earlier predicted theoretically by Kambili *et al.*⁹

The reduction of K_{TH} below the predicted universal value was explained in terms of the scattering of thermal phonons by beam wall surface roughness using a scalar model for the elastic waves.¹⁰ This analysis showed that the thermal conductance K_{TH} depends on the roughness amplitude w and the correlation length ξ , since the analysis was

performed in terms of a Gaussian correlation function $C(x) = w^2 \exp[-(x/\xi)^2]$.⁹ Values of w equal to 22% and ξ equal to about 75% of the width of the conduction pathway gave a good fit to the data of Ref. 8.¹⁰ Although the fits in terms of a Gaussian correlation function are good, it is not clear if a power-law roughness can give similar results and what are their possible implications on K_{TH} . This will be the topic in the present paper. Note also that, the Gaussian correlation function can be considered as a subcase of the stretched exponential correlation function $C(x) = w^2 \exp[-(x/\xi)^{2H}]$ for roughness exponent $H=1$,¹¹ while for power-law roughness we have $0 < H < 1$.¹¹⁻¹³

Furthermore, the expression for the thermal conductance K_{TH} of a suspended mesoscopic beam connecting two thermal reservoirs is given by¹⁰

$$K_{\text{TH}} = \frac{\hbar^2}{K_B T^2} \sum_m \frac{1}{2\pi} \int_{\omega_m}^{\infty} \frac{\omega^2 e^{\beta\hbar\omega}}{(e^{\beta\hbar\omega} - 1)^2} T_m(\omega) d\omega, \quad (1)$$

where ω_m is the cutoff frequency of the m -propagating mode in the suspended beam, and $T_m(\omega)$ is the transmission coefficient.¹⁰ It is assumed here that the thermal transmission occurs along the x -axis with one-dimensional sideways rough boundaries defined perpendicular to the y -axis. If we denote by $y = \zeta(x)$ the sideways roughness fluctuations of the wire (assumed uncorrelated and the same for both sideways walls), L the length, and \tilde{W} the width of the suspended beam, the transmission coefficient is given by¹⁰

$$T_m = e^{-\gamma_m L}, \quad \gamma_m = \sum_n \frac{(q^2 + q_n q_m)^2 N_n^2 N_m^2}{q_n q_m} \langle |\zeta(q)|^2 \rangle, \quad (2)$$

where $\langle |\zeta(q)|^2 \rangle$ is the Fourier transform of the roughness (auto-) correlation function $C(x) = \langle \zeta(x)\zeta(0) \rangle$. We have $q = \omega/c$ with c the velocity of sound and ω the propagating frequency, and $q_m = \sqrt{q^2 - \omega_m^2}$ with $\omega_m = m\pi/\tilde{W}$. Note that $N_n = \sqrt{2/\tilde{W}}$ if $n > 0$, and $N_n = \sqrt{1/\tilde{W}}$ if $n = 0$.¹⁰

For self-affine rough boundaries the correlation function $C(x)$ has the scaling behavior $C(x) \approx w^2 - \rho_{\text{rms}}^2 x^{2H}$ if $x \ll \xi$, and $C(x) = 0$ if $x \gg \xi$ (Refs. 11 and 12) with $\rho_{\text{rms}}^2 \approx w^2 / \xi^{2H}$ a constant. ξ is the in-plane roughness correlation length, $w = \langle \zeta(x)^2 \rangle^{1/2}$ the saturated rms roughness amplitude, and H ($0 < H < 1$) the roughness exponent which characterizes the degree of surface irregularity at small length scales ($x \ll \xi$) so that the smaller the H the more jagged the roughness profile becomes.^{11,12} In this case, $\langle |\zeta(q)|^2 \rangle$ has the scaling behavior $\langle |\zeta(q)|^2 \rangle \propto k^{-1-2H}$ if $q\xi \gg 1$ and $\langle |\zeta(q)|^2 \rangle \propto \text{const}$ if $q\xi \ll 1$. This is described by the simple analytic model^{13,14}

$$\langle |\zeta(q)|^2 \rangle = \frac{w^2 \xi}{(1 + a|q|\xi)^{1+2H}} \quad (3)$$

with $a = (1/H)[1 - (1 + aQ_c \xi)^{-2H}]$ if $0 < H < 1$, and $a = 2 \ln(1 + aQ_c \xi)$ if $H = 0$.¹³ $Q_c = \pi/a_0$ with a_0 of the order of the atomic spacing. For other roughness models see Refs. 10–12.

Our calculations were performed for sound velocity $c = 8250$ m/s, $a_0 = 0.3$ nm, suspended beam length $L = 1000$ nm [assuming $L \gg \xi$ in order to exclude any other finite size dependence of the thermal conductance on the beam length L besides that of the exponential dependence of the transmission coefficient from Eq. (2)], and beam width $\tilde{W} = 167$ nm, which were also used in Ref. 9. Figure 1 shows a comparison of the power-law roughness spectrum $\langle |\zeta(q)|^2 \rangle$ from Eq. (3) with that of the Gaussian roughness or

$$\langle |\zeta(q)|^2 \rangle = w^2 \xi \sqrt{\pi} \exp(-q^2 \xi^2 / 4). \quad (4)$$

From Fig. 1 it can be clearly observed that the Gaussian roughness spectrum $\langle |\zeta(q)|^2 \rangle$ decays much faster than that of the power-law roughness spectrum for the same roughness parameters w , ξ and roughness exponents $H = 1$. This difference implies strong differences for the corresponding thermal conductance between Gaussian and power-law roughness.

Figure 2 shows comparison of the thermal conductance for power-law and Gaussian roughness using the limiting value $H = 1$ in Eq. (3). The calculations were performed for simplicity the case of the zero mode ($m = 0$) contribution. The backscattering amplitude from the lowest mode (mode $m = 0$) is given by the simple formula

$$\gamma_0 = \frac{2}{\tilde{W}^2} \frac{\omega^2}{c^2} \frac{w^2 \xi}{(1 + a[\omega \xi / c])^{1+2H}}. \quad (5)$$

Note that the backscattering amplitude γ_0 has a maximum ($\partial \gamma_0 / \partial \omega = 0$) at a frequency $\omega \approx (a\xi/c)(1 + 2H)$ since $(a\xi/c) \ll 1$. Indeed, at low enough temperatures only the lowest mode ($m = 0$) contributes to the thermal conductance, and only the backscattering of this mode reduces the conductance K_{TH} below the universal value K_U as is shown in Fig. 2. It can also be clearly seen that for Gaussian roughness the minimum is deeper and therefore larger the reduction of the thermal conductance from the universal value K_U (due to phonon scattering by wall roughness) from the case of power-law roughness even for exponents $H = 1$. For both types of roughness we used the values $w = 35$ nm and $\xi = 120$ nm from Ref. 10. These values were also used to fit the

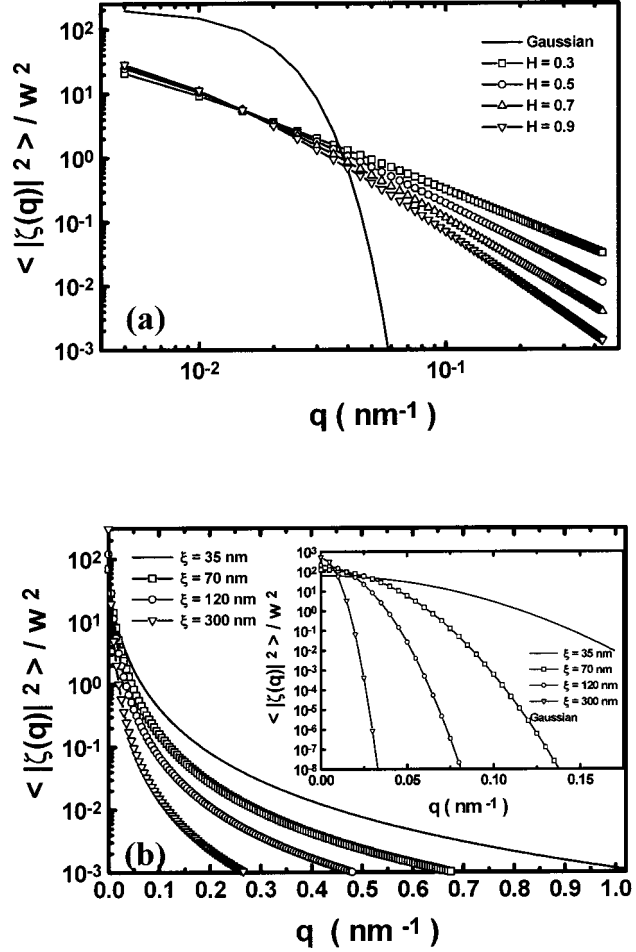


FIG. 1. (a) Calculations of $\langle |\zeta(q)|^2 \rangle$ for Gaussian and power-law roughness, $\xi = 120$ nm, and various roughness exponents H . (b) Calculations of $\langle |\zeta(q)|^2 \rangle$ for power-law and Gaussian (inset) roughness for $H = 0.9$ and various correlation lengths ξ .

experimental data from Ref. 8 in terms of Gaussian roughness in Ref. 10. At any rate, the faster decay of the Gaussian roughness spectrum from that of power law roughness, as it is shown in Fig. 1, minimizes the effect of large wave vectors

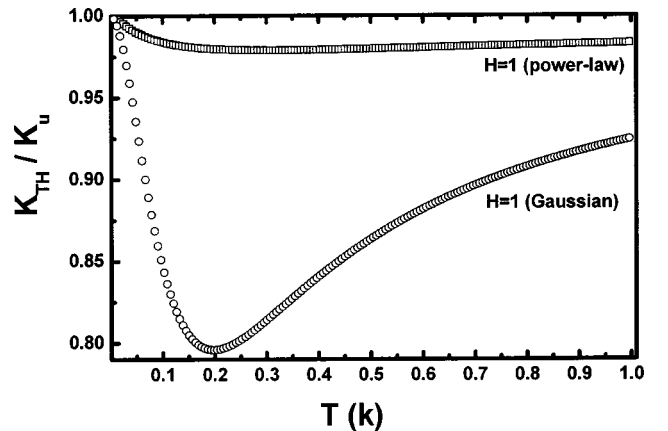


FIG. 2. Calculations of K_{TH} vs temperature T for $w = 35$ nm, $m = 0$, and $\xi = 120$ nm. Comparison of power-law and Gaussian correlation function for $H = 1$.

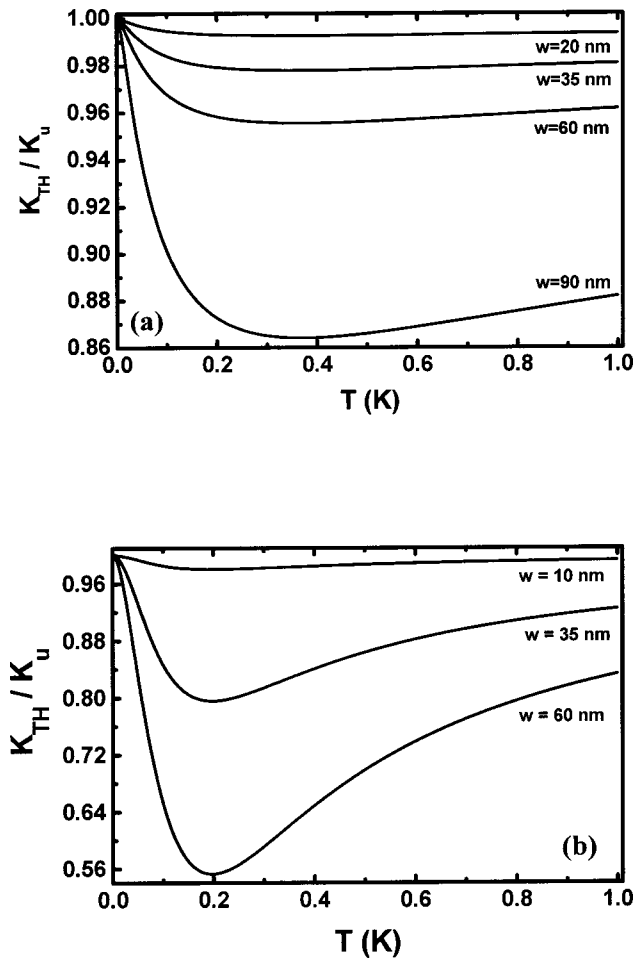


FIG. 3. (a) Calculations of K_{TH} for power-law roughness vs temperature T for $m=0$, $\xi=120$ nm, $H=0.9$, and various roughness amplitudes w . (b) Similar calculations but for Gaussian roughness for $m=0$, $\xi=120$ nm, and various roughness amplitudes w .

q on the transmission coefficient T_m from Eq. (2) and thus on the thermal conductance leading to a deeper minimum (or larger decrease) than that of power-law roughness.

In order to achieve comparable minimum depth for power-law roughness with that of Gaussian roughness, significantly large ratios w/ξ have to be assumed of the order of $w/\xi \sim 1$ [see Fig. 3(a)]. This is rather unphysical since the validity of the present formalism, which is first order perturbation theory, breaks down in the limit of strong roughness and roughness fluctuations comparable to beam width. The influence of the roughness amplitude w is rather significant since from Eq. (5) we have $\gamma_m \sim w^2$ (since $\langle |\zeta(q)|^2 \rangle \sim w^2$) leading to transmission coefficient dependence $T_m \sim e^{-w^2}$. In comparison with the case of Gaussian roughness [Fig. 3(b)], the influence of the rms roughness amplitude on the thermal capacitance shows distinct differences for the case of power-law roughness over the whole range of system temperatures as Fig. 3(a) shows in comparison with Fig. 3(b). Similar is also the behavior of K_{TH} as a function of the roughness correlation length as Fig. 4 shows. In both cases with increasing roughness ratio w/ξ the minimum position shifts to higher temperatures. The differences between Gaussian and power-

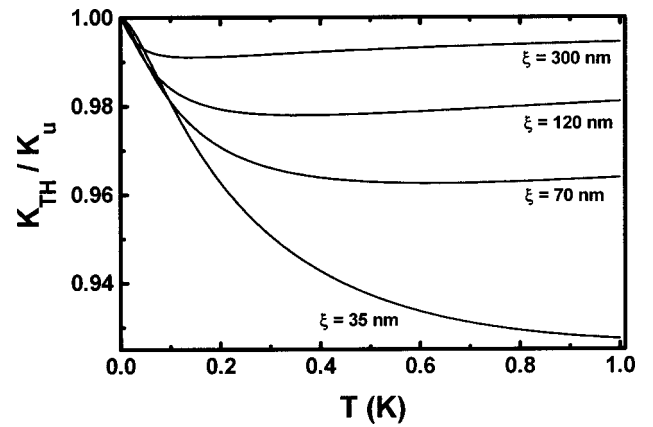


FIG. 4. Calculations of K_{TH} vs temperature T for $w=35$ nm, $m=0$, $H=0.9$, and various roughness correlation lengths ξ .

law roughness are due to the different form of the roughness spectra $\langle |\zeta(q)|^2 \rangle$ as quantitatively shown in Fig. 1 with distinct decay rates at larger wave vectors q .

We should point out that besides the limiting condition $w \ll \tilde{W}$, the limit of strong or weak roughness is determined by the fact that the average local slope

$$\rho_{rms} = \sqrt{\langle |\nabla \zeta|^2 \rangle} = \sqrt{\int_{2\pi/L}^{Q_c} \langle |\zeta(q)|^2 \rangle q^2 dq} \quad (6)$$

to be small or $\rho_{rms} \ll 1$. The latter depends predominantly on the roughness exponent H than the roughness ratio w/ξ .¹⁵ Notably, the changes with decreasing roughness exponent H occur around the temperature $T \sim 0.2$ K, where the minimum is also observed for large roughness exponents $H (> 0.5)$. For temperatures below the temperature where the minimum occurs the effect of the roughness exponent H is rather weak.

At any rate, with decreasing roughness exponent H the minimum of the thermal conductance ceases to exist (Fig. 5), while a continuous decrement with increasing temperature T takes place. This is because there are more favorable conditions for backscattering leading to lower thermal conduc-

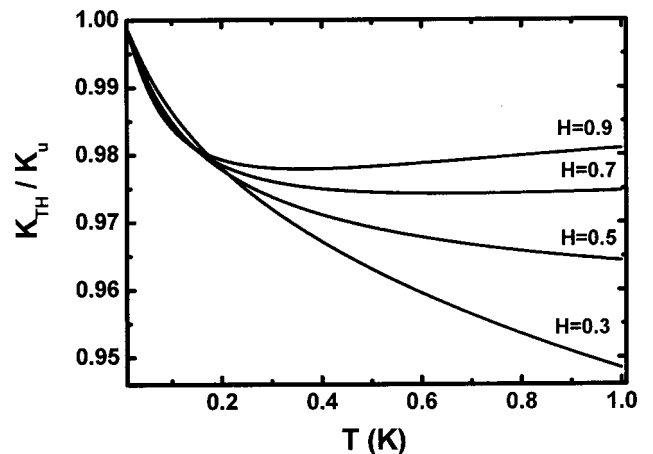


FIG. 5. Calculations of K_{TH} vs temperature T for $w=35$ nm, $m=0$, $\xi=120$ nm, and various roughness exponents H .

tance. This behavior is related with the fact that the roughness spectrum decays slower [Fig. 1(a)] leading to significant contributions from long wavelengths q or equivalently higher frequencies ($q = \omega/c$) in Eqs. (1) and (2). By contrast the fast decaying Gaussian spectrum only allows a limited range of frequencies to contribute to the decrease of the thermal conductance below its ideal value. Additional modes will have similar effect on the thermal conductance since it is the high frequency range that becomes more significant with decreasing roughness exponent H or slower decaying roughness spectrum.

The sub-Kelvin temperature studies ($T < 1$ K) on phonon scattering by wall roughness can be useful in space research that is related to programs (e.g., Constellation-X and XEUS: X-ray Evolving Universe Spectroscopy Mission) which require detectors with challenging specifications.¹⁶ The most promising type of detector is an array of voltage biased superconducting transition edge microcalorimeters operated at sub-Kelvin temperatures.¹⁶ Uniformity of response of arrays of these microcalorimeters is critically dependent on the thermal properties of the materials used. Therefore, it is essential to study the thermal properties of these materials at very low

temperatures (sub-Kelvin temperatures), where the heat conductivity becomes size dependent (through the mean free path of phonons) and phonon scattering by surface roughness plays a fundamental role.

In conclusion, we have compared power-law and Gaussian roughness effects on the thermal conductance of a suspended beam between two reservoirs. Distinct differences occur in between these types of roughness. Indeed, for power-law roughness with low roughness exponents H (< 0.5), the influence of phonon scattering can be rather destructive leading to significant deviations from the universal conductance value for flat beam walls. On the other hand for large roughness exponents ($H > 0.5$) the conductance drop is significantly smaller than that of Gaussian roughness assuming similar roughness ratios w/ξ (indicating weaker phonon scattering). Further studies are necessary to account more correctly for the case of strong roughness or ($\rho_{\text{rms}} \geq 1$) accompanied with precise roughness characterization of beam wall roughness.

I would like to acknowledge useful discussions with Dr. G. Backx.

*Author to whom correspondence should be addressed. Electronic mail: g.palasantzas@phys.rug.nl

¹K. von Klitzing, G. Dorda, and M. Pepper, Phys. Rev. Lett. **45**, 494 (1980).

²B. J. van Wees, H. van Houten, C. W. J. Beenakker, J. G. Williamson, L. P. Kouwenhoven, D. van der Marel, and C. T. Foxon, Phys. Rev. Lett. **60**, 848 (1988).

³D. A. Wharam, T. J. Thornton, R. Newbury, M. Pepper, H. Ahmed, J. E. F. Frost, D. G. Hasko, D. C. Peacock, D. A. Ritchie, and G. A. C. Jones, J. Phys. C **21**, L209 (1988).

⁴R. Landauer, IBM J. Res. Dev. **1**, 223 (1957); R. Landauer, Phys. Lett. **85A**, 91 (1981); G. Kirczenow, Solid State Commun. **68**, 715 (1988); A. Szafer and A. D. Stone, Phys. Rev. Lett. **62**, 300 (1989); E. Haanappel and D. van der Marel, Phys. Rev. B **39**, 5484 (1989); L. Escapa and N. Garcia, J. Phys.: Condens. Matter **1**, 2125 (1989); E. Tekman and S. Ciraci, Phys. Rev. B **39**, 8772 (1989); Y. Avishai and Y. B. Band, *ibid.* **40**, 12 535 (1989); E. Castaño and G. Kirczenow, *ibid.* **45**, 1514 (1992).

⁵B. I. Halperin, Phys. Rev. B **25**, 2185 (1982); M. Büttiker, Phys. Rev. Lett. **57**, 1761 (1986); P. Streda, J. Kucera, and A. H. MacDonald, *ibid.* **59**, 1973 (1987); J. K. Jain and S. A. Kivelson, *ibid.* **60**, 1542 (1988); M. Büttiker, Phys. Rev. B **38**, 9375 (1988).

⁶R. E. Peierls, Ann. Phys. (Paris) **3**, 1055 (1929).

⁷L. G. C. Rego and G. Kirczenow, Phys. Rev. Lett. **81**, 232 (1998).

⁸K. Schwab, E. A. Henriksen, J. M. Worlock, and M. L. Roukes, Nature (London) **404**, 974 (2000).

⁹A. Kambili, G. Fagas, V. I. Fal'ko, and C. J. Lambert, Phys. Rev. B **60**, 15 593 (1999).

¹⁰D. H. Santamore and M. C. Cross, Phys. Rev. B **63**, 184306 (2001).

¹¹S. K. Sinha, E. B. Sirota, S. Garoff, and H. B. Stanley, Phys. Rev. B **38**, 2297 (1988); G. Palasantzas and J. Krim, *ibid.* **48**, 2873 (1993).

¹²Y.-P. Zhao, G.-C. Wang, and T.-M. Lu, *Characterization of Amorphous and Crystalline Rough Surfaces—Principles and Applications*, Experimental Methods in the Physical Science (Academic, New York, 2001), Vol. 37; P. Meakin, *Fractals, Scaling, and Growth Far from Equilibrium* (Cambridge University Press, Cambridge, 1998).

¹³G. Palasantzas, Solid State Commun. **100**, 705 (1996); Phys. Rev. B **50**, 18 670 (1994).

¹⁴For similar models see also by E. L. Church and P. Z. Takacs, Proc. SPIE **615**, 107 (1986); **1530**, 71 (1991).

¹⁵G. Palasantzas, Phys. Rev. E **56**, 1254 (1997); G. Palasantzas and J. Th. M. De Hosson, *ibid.* **67**, 021604 (2003).

¹⁶Z. Moktadir, M. P. Bruijn, R. J. Wiegink, M. Elwenspoek, M. Ridder, and W. A. Mels, Proc. IEEE Sensors 2002, paper 37.3, Orlando, June 11–14, 2002; M. P. Bruijn, W. M. Bergmann Tiest, H. F. C. Hoevers, E. Krouwer, J. van der Kuur, M. L. Riddera, Z. Moktadir, R. Wiegink, D. van Gelder, and M. Elwenspoek, Nucl. Instrum. Methods Phys. Res. A **513**, 143 (2003); see also the programs <http://constellation.gsfc.nasa.gov/> and <http://www.rssd.esa.int/index.php?project=XEUS>.